



HAL
open science

A novel high adhesion cationic waterborne polyurethane for green coating applications

Nathapong Sukhawipat, Nitinart Saetung, Pamela Pasetto, Jean-François Pilard, Sophie Bistac, Anuwat Saetung

► To cite this version:

Nathapong Sukhawipat, Nitinart Saetung, Pamela Pasetto, Jean-François Pilard, Sophie Bistac, et al.. A novel high adhesion cationic waterborne polyurethane for green coating applications. Progress in Organic Coatings, 2020, 148, pp.105854 -. 10.1016/j.porgcoat.2020.105854 . hal-03490500

HAL Id: hal-03490500

<https://hal.science/hal-03490500>

Submitted on 22 Aug 2022

HAL is a multi-disciplinary open access archive for the deposit and dissemination of scientific research documents, whether they are published or not. The documents may come from teaching and research institutions in France or abroad, or from public or private research centers.

L'archive ouverte pluridisciplinaire **HAL**, est destinée au dépôt et à la diffusion de documents scientifiques de niveau recherche, publiés ou non, émanant des établissements d'enseignement et de recherche français ou étrangers, des laboratoires publics ou privés.



Distributed under a Creative Commons Attribution - NonCommercial 4.0 International License

A Novel High Adhesion Cationic Waterborne Polyurethane for Green Coating Applications

Nathapong SUKHAWIPAT^{a,b}, Nitinart SAETUNG^a, Pamela PASETTO^c, Jean-Francois PILARD^{c*},
Sophie BISTAC^d, Anuwat SAETUNG^{e*}

^aDepartment of Materials Science and Technology, Faculty of Science,
Prince of Songkla University, Hatyai campus, Songkhla, Thailand.

^bDivision of Polymer Engineering Technology, Department of Mechanical Engineering Technology,
College of Industrial Technology, King Mongkut's University of Technology North Bangkok,
Bangkok, Thailand

^cInstitut des Molécules et Matériaux du Mans, UMR CNRS 6283,
Le Mans Université, 72085 Le Mans Cedex 9, France.

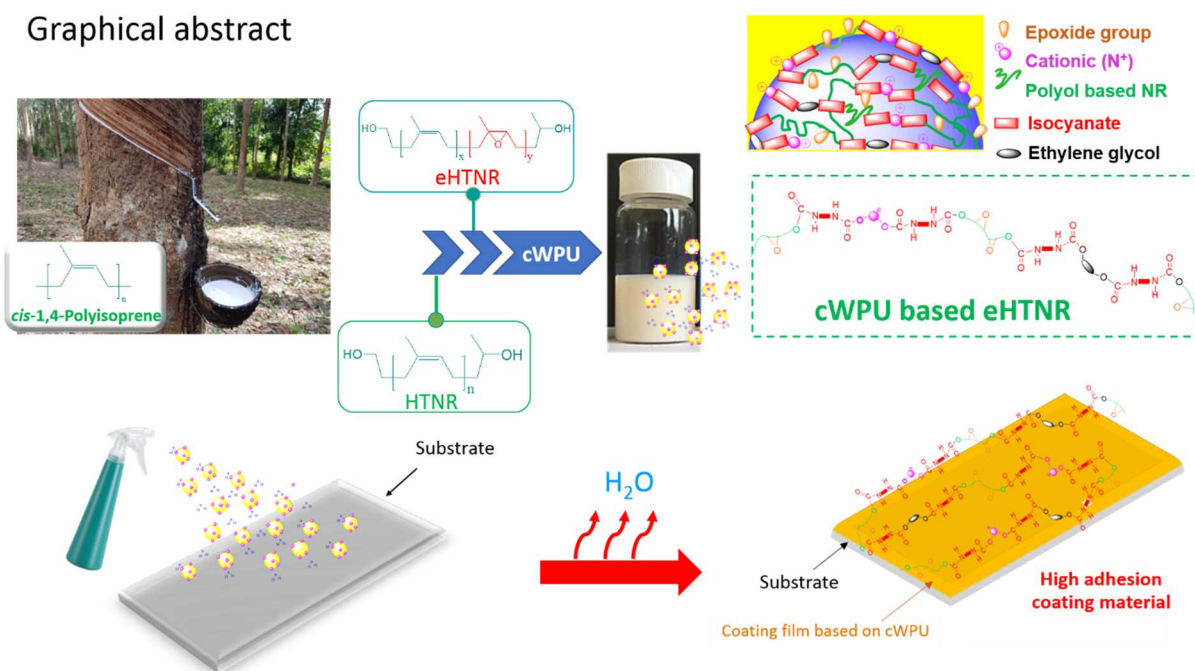
^dUniversité de Haute Alsace, LPIM, 3 rue Alfred Werner 68093 Mulhouse, France.

^eDepartment of Rubber Technology and Polymer Science, Faculty of Science and Technology,
Prince of Songkla University, Pattani campus, Pattani, Thailand

*Corresponding authors E-mail: Jean-Francois PILARD; jean-francois.pilard@univ-lemans.fr

Anuwat SAETUNG; anuwat.s@psu.ac.th

Graphical abstract



Abstract

This report is the first one on a cationic waterborne polyurethane (cWPU) latex based on epoxidized hydroxyl telechelic natural rubber (eHTNR) polyol, providing potential for use as a coating made of renewable resources. A cWPU latex was synthesized by step growth emulsion polymerization from hydroxyl telechelic natural rubber (HTNR) with $M_n = 3,000$ g. mol⁻¹ (with fixed *N*-methyl diethanol amine content of 5.6 wt% and 2,4-toluene diisocyanate (NCO index = 100). The effects of proportion of epoxide units on HTNR polyol from 0 to 30% on preparing cWPU latex were investigated. Chemical structures of HTNR and eHTNR polyol were confirmed by ¹H-NMR spectroscopy. The resulting HTNR and eHTNR polyols present a unimodal size exclusion chromatography trace. The viscosity increased with epoxide fraction. The synthesized cWPU latex based on eHTNR was a stable milky-blue emulsion with well-defined size dispersion. All cWPU-eHTNR films showed good wettability, good chemical resistance, and high thermal stability, improving with the proportion of epoxide units. The mechanical properties of cWPU-eHTNR films were studied from their stress-strain curves. Moreover, the electrical properties were investigated. The cWPU-eHTNR films showed relatively low conductivity. Wettability, chemical resistance, adhesion, thermal stability, and electrical properties of cWPU-HTNR films improved with the proportion of epoxide units on the HTNR polyol. These results demonstrate a new synthesis route to develop cWPU latex based on a biosource, for coating applications.

Keynotes: adhesion, cationic waterborne polyurethane, coating, epoxide group, natural rubber

1. Introduction

Polyurethane (PU) coatings have good flexibility at low temperature, high tensile strength, excellent surface gloss and good dielectric properties. Hence, polyurethanes excel when appropriately applied. Conventionally, a PU coating contains volatile organic solvents in the range 40 – 60% by weight. These solvents are hazardous and irritate eyes, nose, and throat, and cause dizziness and headaches. Moreover, they belong to a group of chemicals that are a major cause of air pollution and environmental problems [1-2]. In the past decade, waterborne polyurethane (WPU) or polyurethane dispersions have been found to have high potential to replace PU with solvent-based coatings that are more environmentally friendly, easy to handle, and non-toxic. [2-4]. There are three classes of WPU – cationic, anionic, and

nonionic – depending on the neutralized charge of emulsifier inserted in the system. It has been reported that cationic WPU)cWPU(latex serves as a unique type of coating with high adhesion properties due to its good dispersion in water, good film-formation ability, and excellent adhesion on many surfaces, such as polymeric or glass substrates]5[.

Most of the polyols used in polyurethane preparation are polyethers and polyesters and normally come from petroleum] 6-9[. To reduce the use of fuel-based polyols, many investigations have tried to modify oil extracted from plants to obtain new types of biosourced polyols for polyurethane preparation, such as soybean oil] 4, 10-11[, Tung oil]12[, or castor oil]13[. However, the physical and mechanical properties are limited by a low molecular weight, and further, vegetable oils are usually employed in food and consumed. To overcome these drawbacks, our research focused on other natural polymer sources, especially natural rubber, a renewable and green material, which has been modified using the reactivity of double bonds along the molecular chains of *cis*-1,4-polyisoprene and has excellent physical properties] 14-15[. In our previous work, cWPU latex was first synthesized and characterized from hydroxyl telechelic natural rubber)HTNR(oligomers, with a molecular weight of about 3000 g. mol^{-1} , used as biosourced polyol, and its mechanical properties as thick films were studied]16[.

There are many reports on improving mechanical properties and adhesion strength of WPU latex. Firstly, nano-filler has been added into the WPU latex system, but there are some limitations regarding usage and storage time. One of such limitations is the decrease of adhesion due to the aggregation of the filler] 17-18[. In another study, the polymer chain structure was modified by grafting/ adding reactive polar groups onto WPU latex, such as acrylate monomer]19-21[or epoxide groups]22[to improve strength and adhesion of WPU film. The crosslinked network formed during acrylate grafting polymerization increased thermal stability and mechanical properties of the resulting miscible grafted lattices, resulting in high performance coating materials. However, the grafting procedure is very complicated, time consuming, and requires chemical agents that may not be environmentally friendly. Also, epoxy resin is used as an adhesive in electrical applications because of its excellent chemical resistance and high thermal stability]23[.

To the best of our knowledge, there are no reports on improving adhesion strength of cWPU latex by inserting epoxide groups in the structure. To address this gap, the present study focused on the chemical modification of the main chain structure of the biosourced polyol)HTNR(. The epoxidized hydroxyl telechelic natural rubber)eHTNR(was prepared

with a starting molecular weight of about 3000 g.mol⁻¹ and with various epoxide contents on the eHTNR polyol backbone.

The eHTNR was used as biosourced polyol to synthesize cWPU latex. The physical, mechanical, thermal stability, electrical and adhesion properties of cWPUs were investigated. As example of a possible real application, the adhesion of the cWPU latex to leather substrate was studied and compared to commercial glues.

2. Materials and Methods

2.1 Materials

Concentrated natural rubber latex with high ammonia percentage (0.7% ammonia, with dry rubber content) DRC (of approximately 60%), and total solids content) TSC (of approximately 62%), was purchased from Yala Latex Industry co., Ltd. (Thailand). Hydrogen peroxide (H₂O₂, 35%) and sodium borohydride (NaBH₄, 98%) were purchased from Ajax Finechem (Unilab®) (Australia). Formic acid (HCOOH, 98%) was purchased from BASF-YPC Company Limited (China). Methyl ethyl ketone solvent (MEK) was purchased from Fisher Scientific UK Limited (England). Periodic acid (H₅IO₆, 99%), 3-chloroperbenzoic acid (mCPBA, 77%), *N*-methyl diethanol amine (NMDEA, 99%), 2,4-toluene diisocyanates (TDI, 98%), and dibutyltindilaurate (DBTDL) were purchased from Sigma-Aldrich (Germany). Acetic acid (CH₃COOH, 95%) and ethylene glycol (EG, 99.5%) were purchased from Carlo Erba (Italy). All reagents were used without further purification. Leather sheets (non-treated) for adhesion testing of the coatings were purchased from Leather shoes community enterprise (Top Plate, Khlong Luang, Pathum Thani) (Thailand).

2.2 Methodology

2.2.1 Preparation of HTNR and eHTNR polyol

Hydroxyl telechelic natural rubber (HTNR) (with molecular weight of 3000 g.mol⁻¹ was obtained from previous work [16]). The eHTNR was prepared from HTNR via controlling epoxidation percentage to 10, 20 or 30%. The reaction was performed in a three-necked round bottom flask equipped with a magnetic stirrer at 0 °C under argon gas atmosphere. HTNR3000 (10 g, 3.33 mmol) was dissolved in dried dichloromethane (0.067 mol.L⁻¹) in the flask and then a solution of *m*-chloroperbenzoic acid (2.538g, 14.7 mmol for 10% epoxide; 5.08 g, 29.4 mmol for 20% epoxide; 7.61 g, 44.10 mmol for 30% epoxide) in dried dichloromethane (50mL) was added dropwise into the reaction flask. The equivalent

mole ratio of mCPBA to isoprene units in HTNR3000 was 0.1, 0.2 or 0.3 for epoxide contents of 10, 20 or 30 %, respectively. The reaction was run for 3 hours. At the end, it was quenched by adding a saturated solution of NaHCO₃)500 mL(, followed by washing with a saturated NaCl aqueous solution) 500 mL(. The mixture was transferred into a separating funnel and the organic phase was rescued and dried with anhydrous magnesium sulfate. The organic solvent was removed under reduced pressure and the oligomers were left in an oven at 40 °C for 3 hours, under vacuum, to get the products with 92% , 91% and 95% yields for 10, 20 and 30% epoxide, respectively.

2.2.2 Preparation of cWPU latex based on eHTNR polyol

We investigated the synthesis of cWPU latex using eHTNR as biosourced polyol with various contents of epoxide group. The reaction was performed in THF at 70 °C under argon, and the mixture of NMDEA and DBTL was added in the reactor equipped with a stirrer)100 rpm(, and TDI was added dropwise into the reaction mixture. After 4 hours, EG was gently dropped into the system for 30 minutes, with stirring rate of 400 rpm. The system was then cooled and neutralized with acetic acid)1.50 equivalent mole of NMDEA(for 1 hour, with a stirring rate of 400 rpm. Deionized water was slowly dropped for 30 minutes, while stirring at a speed of 400 rpm. Finally, the THF was removed under reduced pressure to obtain cWPU-based eHTNR. The formulations of cWPU latex based on eHTNR polyol are summarized in **Table 1**.

Table 1. The formulations of cWPU latex based on eHTNR polyol

Chemical	Recipe (mole)			
	cWPU-HTNR	cWPU-eHTNR10	cWPU-eHTNR20	cWPU-eHTNR30
HTNR	1	1	1	1
NMDEA ^a	1.90	1.97	2.05	2.09
Ethylene glycol	1	1	1	1
TDI	3.90	3.97	4.05	4.09
(NCO index = 100)				

All cWPU latex with a controlled solid content of 16%

2.3 Characterizations of eHTNR polyol

Structure confirmation of eHTNR polyol

MALDI-TOF mass spectrometry was performed on a Bruker UltraFlex II instrument equipped with a nitrogen laser operating at 337 nm, pulsed ion extraction source and reflection. Spectra were recorded in the reflection mode with an acceleration voltage of 19 kV and a delay of 200 ns. 1000 single shot acquisitions were summed to give the spectra and the data were analyzed using Bruker FlexAnalysis and Polytools software. Samples were prepared by dissolving the matrix trans-2-[3-(4-tert-Butylphenyl(-2-methyl-2-propeny-lidene[malononitrile) DCTB(in dichloromethane solvent and mixing with the polymer) 10 mg.mL⁻¹(and the cationizing agent silver trifluoroacetate)AgTFA(in the ratio 1:20:1.

Molecular weight determination

Size Exclusion Chromatography. Number-average molecular weight (M_n) and dispersity)D(were measured by size exclusion chromatography)SEC(with THF as eluent)1 mL.min⁻¹(, at 35°C, on a Waters® chain 2707 autosampler equipped with a 1515 Isocratic Pump and a guard column)Styragel 30x4.6 mm(connected to a column)Styragel HR2 + HR4, 300x7.8mm(. The Waters® 2996 PDA and Waters® 2414 Refractive Index Detector were used. Calibration was performed with polystyrene)PS(standards in the range from 580 g.mol⁻¹ to 483000 g.mol⁻¹. The molecular weights of the oligoisoprenes were corrected using Benoit factor equal to 0.67.

Viscosity measurement

Viscosity measurements were carried out with an AR 2000 TA Instruments with cone head of 20 mm and 3°58'. A flow ramp was used with 5 min time to adjust temperature, then 5 points per decade were recorded from 0.01 to 100 s⁻¹ during 120 seconds.

2.4 Characterizations of cWPU latex

Total solids content

The total solids content of cWPU latex was calculated from differential weight before and after drying. About 1 g of cWPU latex was placed in an aluminum tray and dried in an air

oven at 100 °C until constant weight. The solids content (TSC) is calculated as average of 3 samples as follows:

$$TSC (\%) = \frac{W_i - W_x}{W_i} \quad (1)$$

where W_i is the weight of the initial cWPU latex and W_x is the weight after drying the sample.

Morphology

The morphology assessment of synthesized cWPU latex was done by transmission electron microscope (TEM) imaging on a model JEOL JEM-2010 operated at 160 kV. The samples were diluted with deionized water and stained with 2% osmium tetroxide solution on the coated side of a 200-mesh copper grid, and allowed to dry before imaging.

Particle Size Distribution

The particle size distributions of synthesized cWPU latex were characterized with a Nano-ZS particle sizer (Malvern Instruments Company, UK) at room temperature. The latexes were diluted to 1% before testing, without further filtration. The particle size was calculated as average of 5 times for each formulation.

2.5 Characterizations of cWPU film

Film preparation

Films from all the samples were prepared by casting into Teflon molds with cavity size 5 cm x 11 cm x 0.3 mm. After casting the molds were left at room temperature for 3 days, then the emulsion solutions were dried in an oven at 70 °C for 24 hours.

¹H Nuclear magnetic resonance (¹H-NMR) spectroscopy

¹H Nuclear magnetic resonance (¹H-NMR) spectra were recorded on a Bruker® 400 Fourier transform spectrometer (400 MHz). The samples were dissolved in chloroform-d ($CDCl_3$) and methanol-d (CD_3OD), using tetramethylsilane as an internal standard (TMS, $\delta = 0$ ppm). The percentage of epoxide units on eHTNR was calculated as follows:

$$Epoxide (\%) = \frac{I_{2.69}}{I_{2.69} + I_{5.14}} \times 100 \quad (2)$$

where $I_{2.69}$ is the peak integration at 2.69 ppm (CH epoxide)

$I_{5.14}$ is the peak integration at 5.14 ppm ($C=CH$ isoprene)

Molecular weights (M_n) of eHTNR were calculated as follows:

$$M_n (g \cdot mol^{-1}) = \left(\frac{I_{5.14}}{I_{3.69}} \times 68 \right) + \left(\frac{I_{2.69}}{I_{3.69}} \times 84 \right) + 104 \quad)3($$

where $I_{2.69}$ is the peak integration at 2.69 ppm (CH epoxide)

$I_{3.69}$ is the peak integration at 3.69 ppm ($CHOH$)

$I_{5.14}$ is the peak integration at 5.14 ppm ($C=CH$ isoprene)

Contact angle measurement

Wettability properties were determined by contact angle measurements using a Drop shape analyser, KRUSS)Model: DSA100(with sessile drop method. The contact angles were measured with three test liquids: deionized water, diiodomethane, and bromomethane. Surface energy was calculated from the Owen-Wendt theory using equation)4(. Substituting this expression in the Young equation, the polar and the dispersive parts of the solid's surface energy can be determined from the regression line in a suitable plot.

$$\frac{\sigma_L(\cos\theta+1)}{2\sqrt{\sigma_L^D}} = \sqrt{\sigma_S^P} \cdot \frac{\sqrt{\sigma_L^P}}{\sqrt{\sigma_L^D}} + \sqrt{\sigma_S^D} \quad)4($$

Here θ is the contact angle, σ_L = overall surface tension of the wetting liquid, σ_L^D = dispersive component of the surface tension of the wetting liquid, $\sqrt{\sigma_S^D}$ = polar component of the surface tension of the wetting liquid, $\sqrt{\sigma_S^P}$ = dispersive component of the surface energy of the solid, and $\sqrt{\sigma_L^P}$ = polar component of the surface energy of the solid.

Scanning electron microscopy (SEM)

The fracture surface photographs of the samples from tensile testing were taken by scanning electron microscope (SEM) using JSM-6510LV (JEOL, Japan) in conditions of high vacuum and high voltage at 20.00 kV. All the samples were gold coated before imaging.

Swelling test

The samples were prepared to 6 mm diameter, and were immersed into three types of solvents, dimethylformamide (DMF), toluene, and tetrahydrofuran (THF), for 24 hours. The swelling was determined from linear dimension change during immersion.

$$\text{Swelling (\%)} = \frac{D_{\text{swelling}} - D_{\text{initial}}}{D_{\text{initial}}} \times 100 \quad (5)$$

Here D_{initial} is the diameter of cWPU film before testing (mm), and D_{swelling} is the diameter of cWPU film after testing (mm).

Water absorption

Water absorption behaviors were assessed by weighting each sample film (1 cm × 1 cm) before and after immersion in distilled water for one week. The water absorption was calculated as average of 5 samples for each formulation as follows:

$$\text{Water absorption (\%)} = \frac{W_a - W_b}{W_b} \times 100 \quad (6)$$

Here W_a is the weight of the film after immersion and W_b is the initial weight of the dry film.

Tensile strength

Tensile testing samples of cWPU films were prepared following ISO37 standard with die type 2. The films were characterized by using an Instron machine (Model 3365). The apparatus was equipped with a 100 N load cell and the extensor grips included a laser sensor for checking the elongation, measured with crosshead speed of 100 mm.min⁻¹.

Differential scanning calorimetry (DSC)

The thermal properties of cWPU films were measured with TA instruments DSC Q100. The aluminum pan was loaded with a starting sample weight of about 10 mg and the run was under nitrogen atmosphere (nitrogen flow = 100 mL.min⁻¹) with a heating rate of 10 °C.min⁻¹ from -100 °C to 100 °C. The thermal history was erased with the first run, and then the second heating scan was used to determine the correct glass transition temperature (T_g) of synthesized cWPU.

Thermogravimetric analysis (TGA)

Thermal stability of the cWPU films was characterized by TGA from room temperature to 600 °C, at a heating rate of 10 °C min⁻¹ under nitrogen atmosphere, using approximately 10 mg samples. The activation energy of degradation (E_a) was calculated from the Horowitz–Metzger [24] equation as follows.

$$\ln[-\ln(1 - \alpha)] = \frac{-E_a \theta}{RT_s^2} + C \quad (7)$$

where α represents the fraction of weight loss during degradation in function of time, $\theta = (T - T_s)$, where T_s is the temperature corresponding to the peak location in the DTG curve, E_a is the activation energy of degradation to be estimated, and R is the gas constant (8.314 J K⁻¹ mol⁻¹). The plot of $\ln[-\ln(1 - \alpha)]$ versus θ , in the range of DTG peaks, theoretically gives a straight line. By the least-squares method, the kinetic parameters of thermal degradation can be estimated from the slope and intercept of a straight-line fit [21, 25-26].

Dynamic mechanical thermal analysis (DMTA)

Dynamic mechanical analyses of the cWPU films were carried out with a DMTA (Anton Paar MCR302 model) in tensile mode at a frequency of 1 Hz and 0.01% strain with a heating rate of 38 °C.min⁻¹ by scanning temperatures from -100 °C to 150 °C. Tensile storage modulus (G'), loss modulus (G''), and loss factor ($\tan \delta$) as the ratio of loss modulus to storage modulus (G''/G') were used to quantify the elastic and viscous behaviours of viscoelastic materials under deformation.

Electrical properties

Electrical properties of cWPU films were measured with an LCR meter (HIOKI IM3533-01). The film size was 1 cm x 1 cm for 3 replicates of one sample type. The frequency of measurement was varied from 0 to 100 kHz at room temperature.

2.6 Adhesion properties of cWPU latex based eHTNR

T-Peel Test

Before bonding, real cow leather was degreased with a rag containing acetone] 18[. All cWPU latex samples with a controlled weight of 500 mg were directly applied on the real cow leather surface and pressed at 70 °C, then allowed to set overnight. The assembly was pressed with 1 kg/50 cm² over the adhesive area on sample. For each case, 5 replicates were prepared.

T-peel tests were carried out at constant speed of 10 mm.min⁻¹ using a Universal Testing Machine)Model M500-30AT(in tensile mode in compliance with ISO 11339.

Adhesive tests were also performed on the following commercial adhesives for comparison:

Commercial A: Nouveau SADER)Non-solvent adhesive and coating(

Commercial B: Movil Multikol Transparent)Solvent based adhesive and coating(

3. Results and Discussion

3.1 eHTNR polyol properties

The chemical structures of biosourced polyol based on HTNR, eHTNR and films of cWPU were characterized by ¹H-NMR spectroscopy, with results shown in **Figure 1**. Regarding the characteristic peaks, the signals of isoprene unit were observed in all samples at 5.14(**d**), 2.07(**b, f**), 1.67(**c**), and 1.25(**h**) ppm corresponding to)-CH₂)CH₃(C=CHCH₂-(,)-CH₂)CH₃(C=CHCH₂-(,)-CH₂)CH₃(C=CH-(, and)-CH₂)CH₃(CHO-(, respectively. Moreover, the intense signals at 3.69(**a**) and 3.83(**g**) correspond to methylene proton and methane proton adjacent to hydroxyl end group]16, 27-28[. This indicates that the synthesis of biosourced polyol from natural rubber was successful. In addition, ¹H-NMR spectra of eHTNR and films of cWPU showed new signals at 2.6–2.8(**k**) ppm corresponding to methine proton)-CH₂)CH₃(C)O(CHCH₂-(adjacent to epoxide group. The percentage of epoxide units in eHTNR polyol can be estimated as the ratio of integral peak area of methine proton adjacent to oxirane unit at 2.69 (**k**) ppm to area for vinylic protons of polyisoprene unit at 5.14(**d**) ppm, as in equation)2(. The resulting percentages of epoxide units were about 12, 22, and 32% for eHTNR10, eHTNR20, and eHTNR30, respectively. This confirms that epoxide units were formed in the main chain of eHTNR polyol.

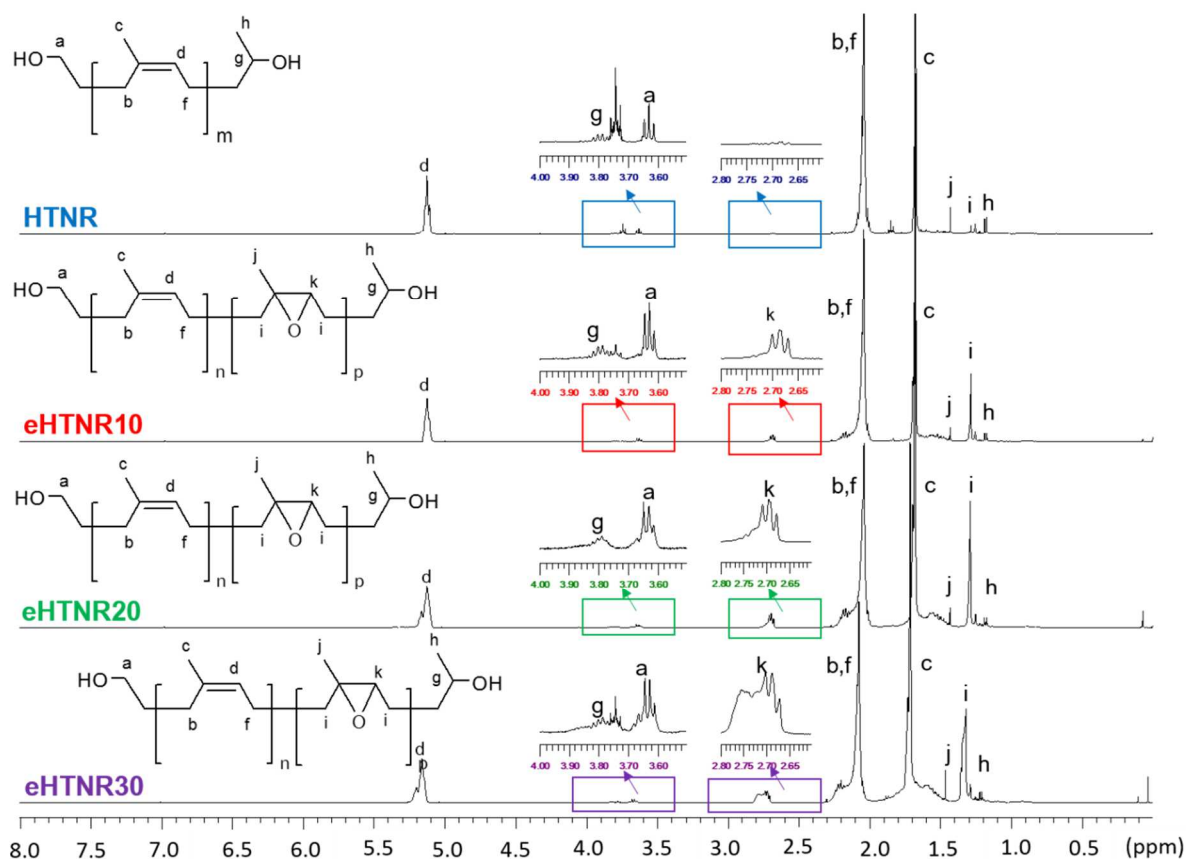


Figure 1. $^1\text{H-NMR}$ spectra of HTNR, eHTNR30 and cWPU-eHTNR30.

The number average molecular weight ($M_{n,cal}$) was calculated based on $^1\text{H-NMR}$ spectroscopy. The integral area of the vinylic protons of isoprene repeat unit at 5.14 (*d*) ppm to methylene proton at 3.69 (*a*) adjacent to hydroxyl group of chain end and the integral area of methine proton adjacent to oxirane repeat unit at 2.69 (*k*) ppm to 3.69 (*a*) adjacent to hydroxyl group of chain, were exploited according to equation) 3(. The ($M_{n,cal}$) was calculated as 3000, 3200, 3300, and 3400 $\text{g}\cdot\text{mol}^{-1}$ for eHTNR10, eHTNR20, and eHTNR30, respectively.

Table 2. Features of eHTNR with various epoxide contents.

Sample	Epoxidation extent (%)	($M_{n,cal}$))g.mol ⁻¹ (($M_{n,SEC}$))g.mol ⁻¹ (D	Viscosity ^a (Pa.s)
HTNR3000	0	3000	3600	2.05	1.97
eHTNR10	12	3200	3800	1.98	3.82
eHTNR20	22	3300	3900	2.05	4.21
eHTNR30	32	3400	4200	1.95	8.02

^a applied shear rate of 100 s⁻¹ and the viscosity was recorded temperature of 50 °C

Furthermore, the number average molecular weight ($M_{n,SEC}$) and D of eHTNR polyol were determined by SEC, as shown in **Table 2**. The estimates of ($M_{n,SEC}$) obtained from SEC using Benoit factor 0.67 were 3600, 3800, 3900 and 4200 g. mol⁻¹ for HTNR, eHTNR10, eHTNR20, and eHTNR30, respectively. The estimates from SEC are close to those from ¹H-NMR. The SEC traces of all eHTNR show a unimodal curve as shown in **Figure 2**. The average molecular weight and polydispersity of eHTNR10 and eHTNR20 show no statistical difference while the eHTNR30 was slightly higher than the average molecular weight, which is due to the absence of a proportion of low molecular weight. This may be attributed to intermolecular reactions between the epoxide groups increasing molecular weight by making larger molecules, more so with more epoxide units. This matches the viscosity results for eHTNRs at 50 °C at various shear rates, shown in **Figure 3**. As the extent of epoxidation increased, so did the viscosity. Clearly the proportion of epoxide units affects physical properties of the eHTNR polyol.

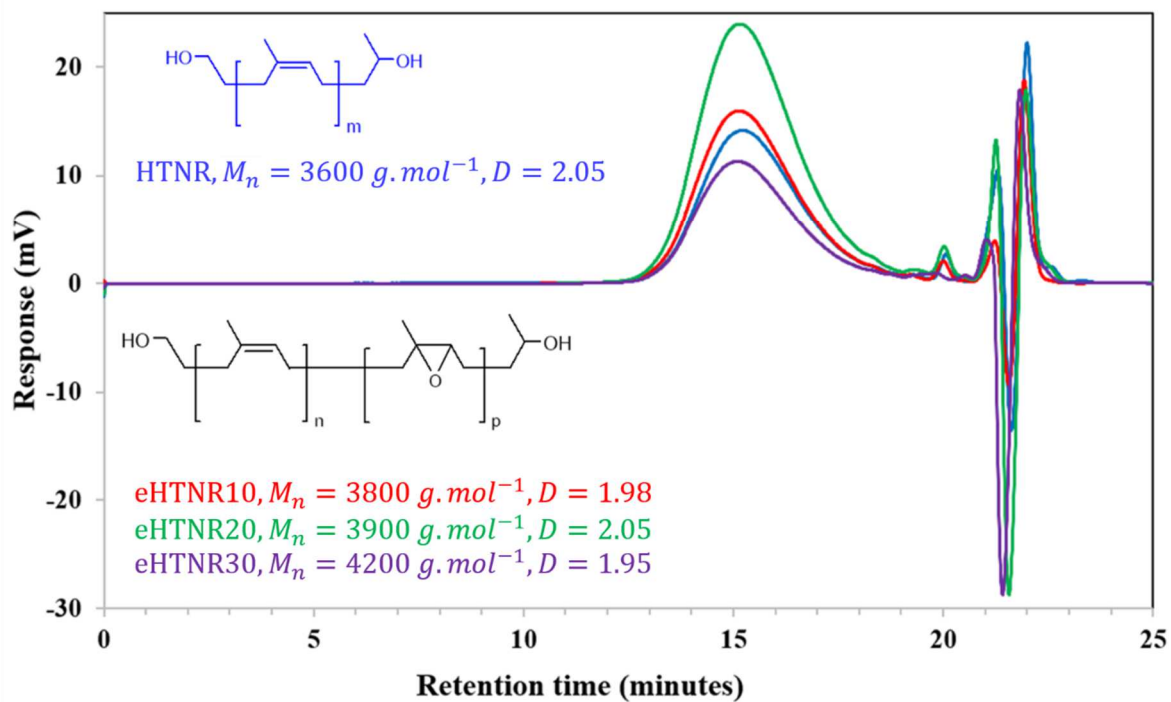


Figure 2. Size exclusion chromatograms and dispersity of eHTNR with different epoxide contents.

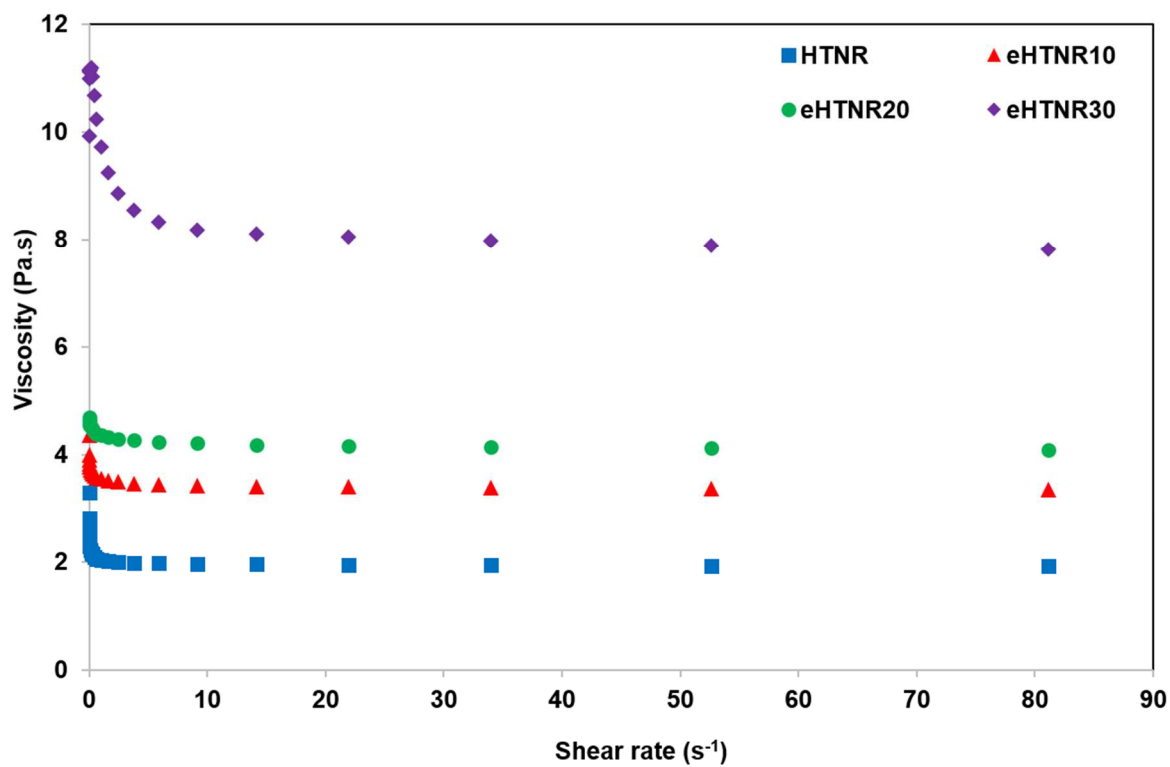


Figure 3. Viscosity of eHTNR polyol.

3.2 cWPU latex properties

cWPU latex based on eHTNR were successfully prepared by step-growth polymerization. The stable cWPU latex had a milky-yellow appearance at 16% TSC and had pH of 4.20 – 4.28. All the cWPU-eHTNR latex showed well-dispersed particles for more than 6 months, indicating a long shelf life.

Table 3. Physical properties of cWPU-eHTNR latex

Sample	TSC (%)	pH	Particle size		Zeta Potential (mV)
			Average Size (nm)	PDI	
cWPU-HTNR	16.67	4.20	76	0.44	+71
cWPU-eHTNR10	17.76	4.22	79	0.28	+57
cWPU-eHTNR20	18.01	4.24	94	0.11	+54
cWPU-eHTNR30	14.55	4.28	188	0.53	+50

The particle sizes of all cWPU-eHTNR latex samples were larger than that of cWPU-HTNR latex and increased with proportion of epoxide units as shown in **Figure 4**. The particle size could depend on the viscosity of eHTNR polyol. The particle size and PDI of the cWPU-eHTNR latex increased from 79 to 188 nm and from 0.44 to 0.52, respectively. The eHTNR_30 polyol with high viscosity gave a highly viscous prepolymer, so that the shear forces were unable to breakdown the larger particles to smaller ones. The Zeta potentials of cWPU-HTNR and cWPU-eHTNR latex are also shown in **Table 3**. All the cWPU latex have positive charge from neutralizing NMDEA with acetic acid. It was found that the synthesized cWPU latex particles were stable and had a high density of positive charges on their surfaces. The zeta potential decreased from +71 to +50 mV with increasing epoxide proportion units. In general, low zeta potentials)lower + 30 mV(lead to particles coagulation or flocculation due to the Van der Waals attractive forces, which act upon them leading to larger particle size]29[, as shown in **Figure 5**. However, all the cWPU-eHTNR latex have the zeta potential more than + 30 mV and are considered to have sufficient repulsive force to attain good physical colloidal stability.

Moreover, particle shape and particle size of cWPU-eHTNR latex were also visualized by TEM. The dark cWPU phases in TEM images are due to contrast staining with OsO₄, as it interacts with the carbon-carbon double bonds of repeating isoprene units. Synthesized

cWPU particles displayed a spherical shape and a possible model of cWPUs-eHTNR latex is presented in **Figure 6**. From TEM results, the particle sizes of cWPU from HTNR, eHTNR10, eHTNR20, and eHTNR30 were about 50, 70, 90, and 190 nm, respectively. These data clearly show that the cWPU latex based on eHTNR was successfully prepared *via* emulsion polymerization.

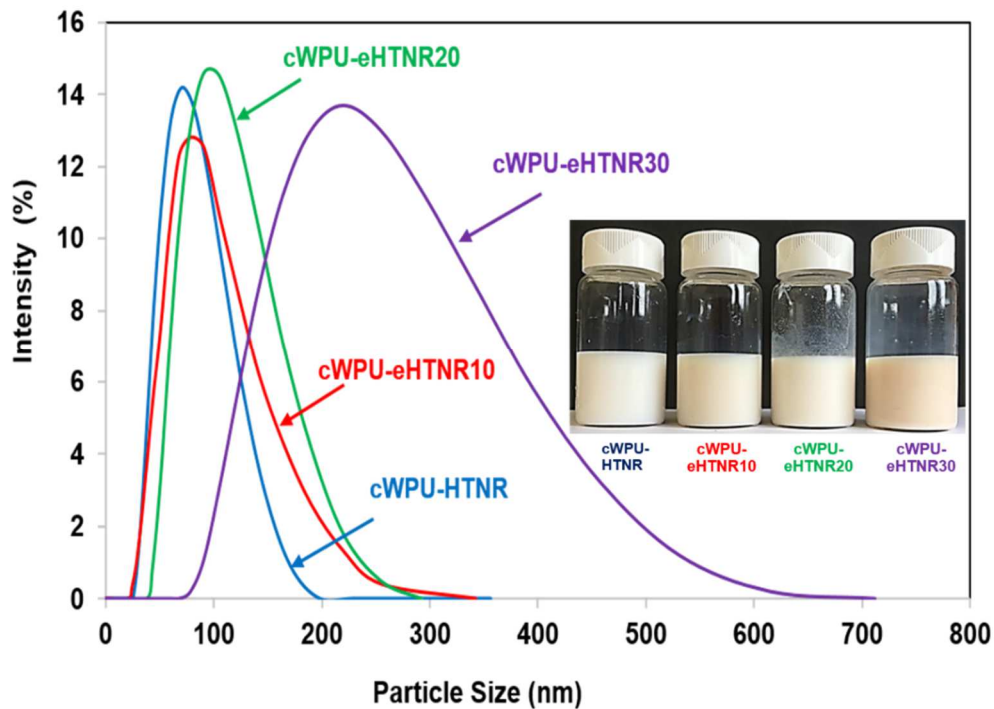


Figure 4. Particle size distributions in a series of cWPU-eHTNR latex

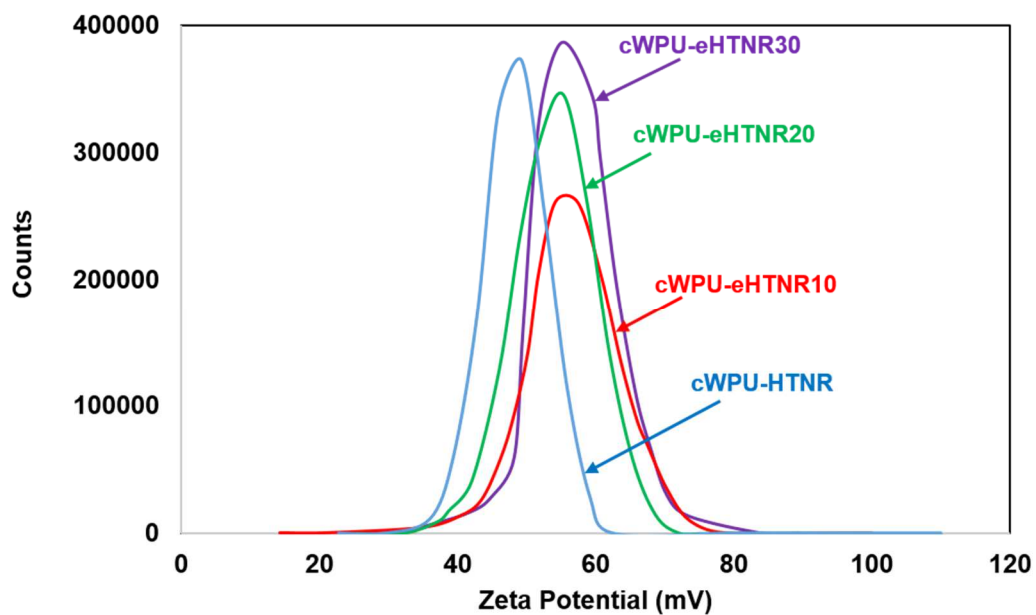


Figure 5. Zeta potential in a series of cWPU-eHTNR latex

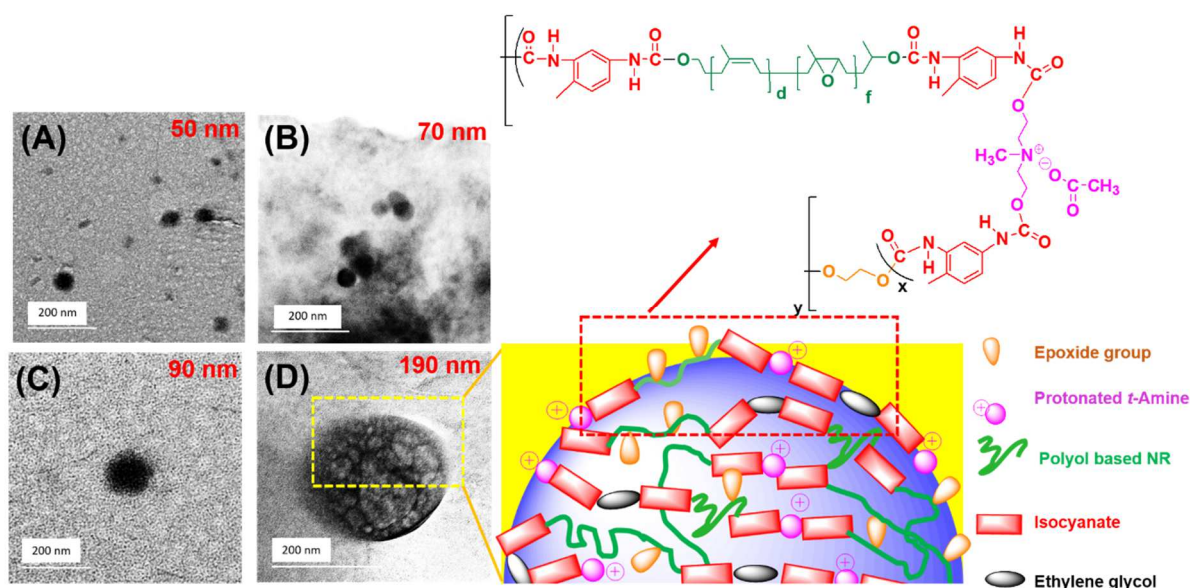


Figure 6. TEM images of cWPU, (A) cWPU-HTNR, (B) cWPU-eHTNR10, (C) cWPU-eHTNR20, (D) cWPU-eHTNR30, and (E) schematic model of a cWPU-eHTNR colloidal particle

3.3 cWPU film properties

The cWPU films, with thickness of 0.1 cm, showed light yellow color with high transparency, and highly glossy surfaces in all cases. These are both important properties for a good coating.

3.3.1 Water absorption and swelling index

The effects of proportion of epoxide units in cWPU-eHTNR films on water absorption are presented in **Table 3**. In the first five days, water absorption increased from 3.7 to 8.7%, as epoxide unit ratio increased from 0 to 30%wt, and after 5 days the absorption slightly increased towards saturation, as shown in **Figure 7**. The polarity of the cWPU-eHTNR films increased with proportion of polar epoxide units on the hydrophobic polyisoprene chains. Thus, cWPU-eHTNR film had more hydrophilic hard segments leading to slightly increased water absorption)less than 10% (. Also, the swelling indexes of all cWPU-eHTNR films were determined in the polar solvents)THF and DMF(and the non-polar solvent)Toluene(. The cWPU-eHTNR films were soluble in THF and DMF after 24 h, so unfortunately we could not determine swelling indexes. The swelling degrees of cWPU films in toluene were 331, 300, 240, and 138% , decreasing with epoxidation level of the

cWPU backbone. This confirms that the polarity of cWPU-eHTNR films was improved by epoxide units on the main chain.

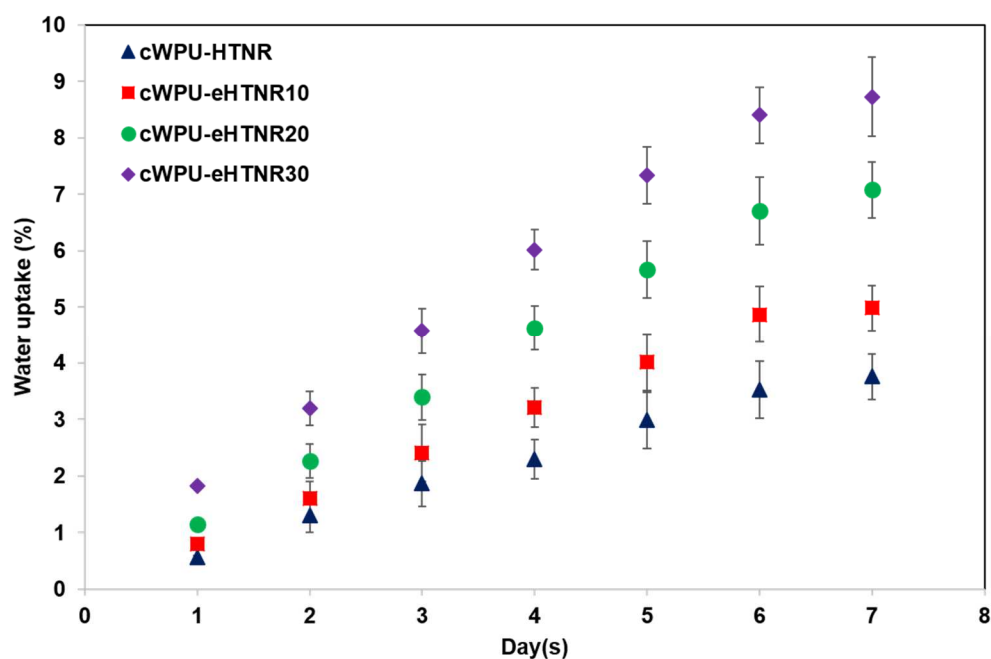


Figure 7. Water absorption in a series of cWPU-eHTNR films

3.3.2 Contact angle and surface energy of cWPU-eHTNR films

Surface wettability is an important property of polymer materials for coating applications. A high proportion of epoxide units) cWPU-eHTNR30(gave the lowest 51° contact angle and highest surface 54.4 mN/ m surface free energy, indicating the most hydrophilic surface) polar component(as shown in **Figure 8**. Theoretically, a high surface energy induces improved wettability and adhesion with any material]30[. For comparison, in 2008, Lin Y. H. *et al.* synthesized fluorinated poly(urethane-acrylate(and they reported that the surface energies were in the range 19 – 38 mN/m]31[. In 2011, Hwang H-D and Kim H-J studied fluorinated polycarbonate-based polyurethane dispersions of anionic type. The surface energy of those WPU films were in the range 20 – 50 mN/m]32[. In 2013, Çanak T. Ç. and Serhatl İ. E. synthesized fluorinated urethane acrylate for coating applications. Surface energy of their prepared polyurethane was in the range 22 – 39 mN/m]33[. In 2017, Zheng G. *et al.* synthesized anionic WPU latex and studied the surface properties. The study reported that the surface energy of WPU films was about 19 – 37 mN/m]34[. In these literature data, the surface energies of WPU films were lower than of the cWPU-eHTNR films in this current work. Therefore, these prepared cWPU latex are suitable for coating

applications due to high surface tension and high wettability. From this result, it can be concluded that the prepared cWPU-eHTNR latex is easily spread and coated on a substrate surface, which is good for coating uses.

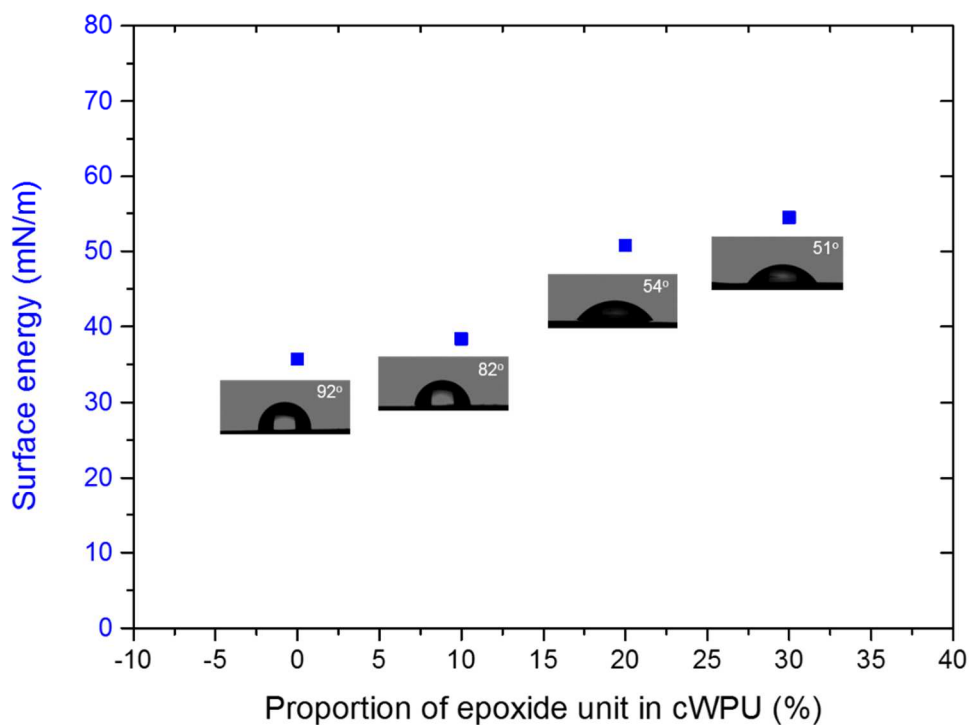


Figure 8 Surface energy and contact angle with deionized water in a series of cWPU-eHTNR films

3.3.3 Tensile properties

Stress-strain curves of cWPU-eHTNR film demonstrate tough plastic behavior increasing with the proportion of epoxide units on the backbone, as shown in **Figure 9**. The Young's modulus of cWPU-eHTNR films continuously increased with the proportion of epoxide units from 1.45 to 2.75 N/mm². However, the rank order by tensile strength had cWPU-eHTNR10 film as the highest followed by cWPU-HTNR, cWPU-eHTNR20 and cWPU-eHTNR30 films, at 7.32, 9.65, 4.34, and 2.35 N/mm², respectively. On increasing the proportion of epoxide units to more than 10 % on the main chain caused typical rigid and brittle plastic behavior with low elongation, so that cWPU-eHTNR20 and cWPU-eHTNR30 films had low tensile strengths. According to the SEM images in **Figure 10**, the cWPU-eHTNR10 film was much rougher than the cWPU-HTNR, cWPU-eHTNR20 and cWPU-

eHTNR30 films. This is associated with the tensile results. The cWPU film with 10% epoxide units on the main chain had the best tensile strength among the cases tested.

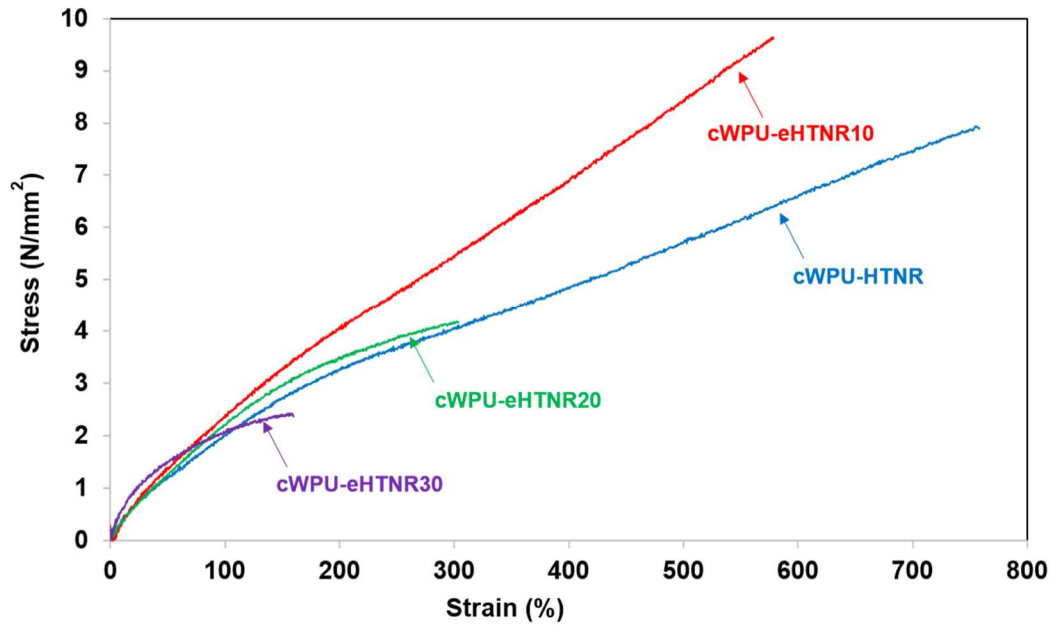


Figure 9. Stress-strain curves in a series of cWPU-eHTNR films

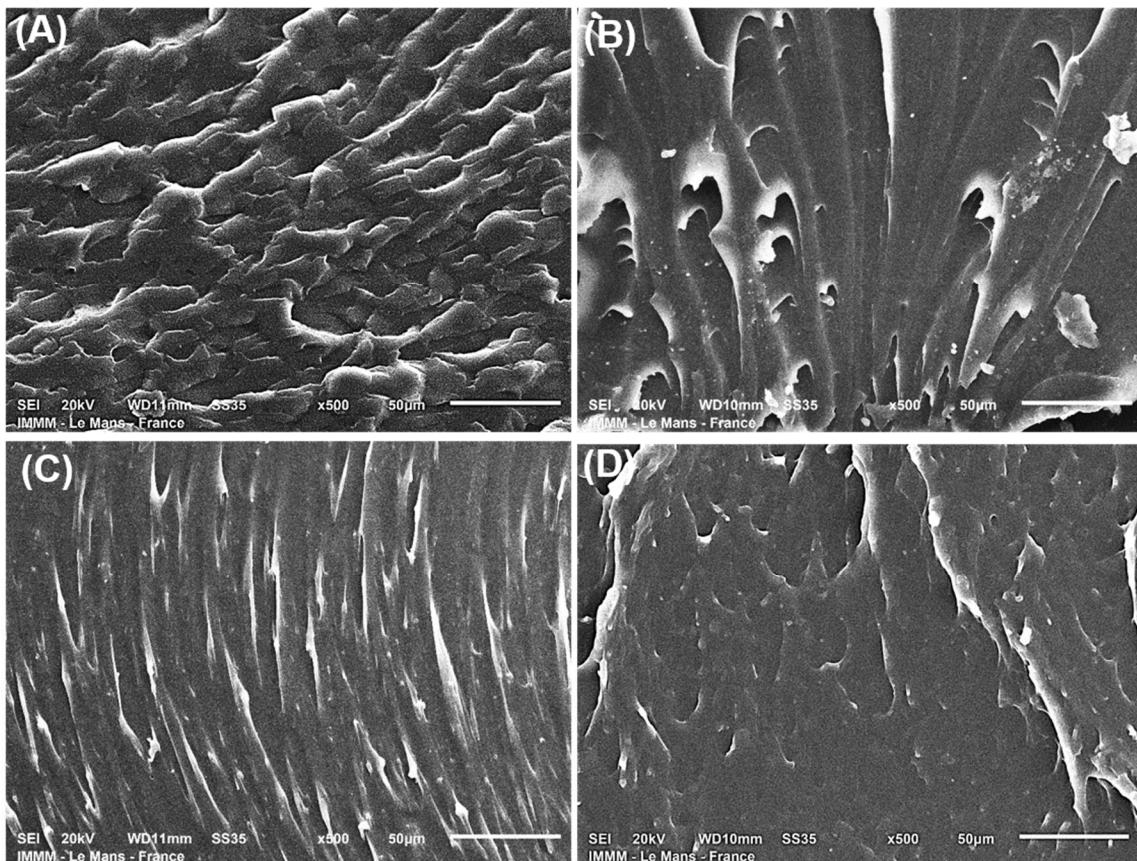


Figure 10. SEM images of cWPU films cross-sections from tensile testing –)A(cWPU-HTNR,)B(cWPU-eHTNR10,)C(cWPU-eHTNR20, and)D(cWPU-eHTNR30

3.3.4 Thermal properties

Thermal degradation of cWPU-eHTNR films was studied by TGA and DTG; the results are summarized in **Table 4**. The DTG curves of cWPU-eHTNR films showed two decomposition steps, seen in **Figure 11**. The first one had T_{max} in the temperature range 208 – 211 °C and is attributed to the decomposition of hard segments at urethane linkages, allophanate and biurate bonding, and also to the loss of carbon dioxide from urethane. The second decomposition step with T_{max} in 370 – 380 °C was from the degradation of natural rubber main chains in cWPU-eHTNR film. The thermogravimetric curve of cWPU film with high proportion of epoxide units is shifted to a higher T_{max} than cWPU-HTNR film. This is because of the physical hydrogen bonding established by urethane linkages and epoxide groups in the main chain, leading to more intra- and intermolecular chain interactions]35[and improving thermal stability of cWPU-eHTNR film. These results match the activation energy of degradation shown in **Table 4**. The cWPU-eHTNR30 film required the highest energy to decompose the hard segments in the first step, whereas in the second decomposition step, cWPU-eHTNR30 film required the least energy to decompose the soft segments. These results confirm that the thermal stability of cWPU film was improved by chemically modifying double bonds in the main chain to epoxide functional groups.

Table 4. Thermal properties results of cWPU films from different eHTNR.

Sample	T_{max} (°C) from TGA		E_a of Degradation (kJ.mol ⁻¹)		T_g (°C)	
	1 st step	2 nd step	1 st step	2 nd step	DSC	DMTA
cWPU-HTNR	211.1	377.2	28.07	60.13	-59.4	-55.2
cWPU-eHTNR10	209.3	379.5	23.65	87.83	-49.9	-48.9
cWPU-eHTNR20	222.1	381.2	23.65	58.38	-42.9	-41.2
cWPU-eHTNR30	208.7	388.0	30.50	58.87	-39.3	-39.6

The DSC curves of all cWPU-eHTNR film showed a single glass transition temperature) T_g (as seen in **Figure 12**. The cWPU films with higher proportion of epoxide units had T_g significantly moved toward higher values, in the sequence -59.4, -44.9, -42.7,

and $-39.3\text{ }^{\circ}\text{C}$. This shift is expected since the introduction of epoxide units and more urethane linkages reduced mobility of the polyisoprene backbone, increasing T_g . This is additional corroboration of successful synthesis of cWPU latex based on eHTNR polyol.

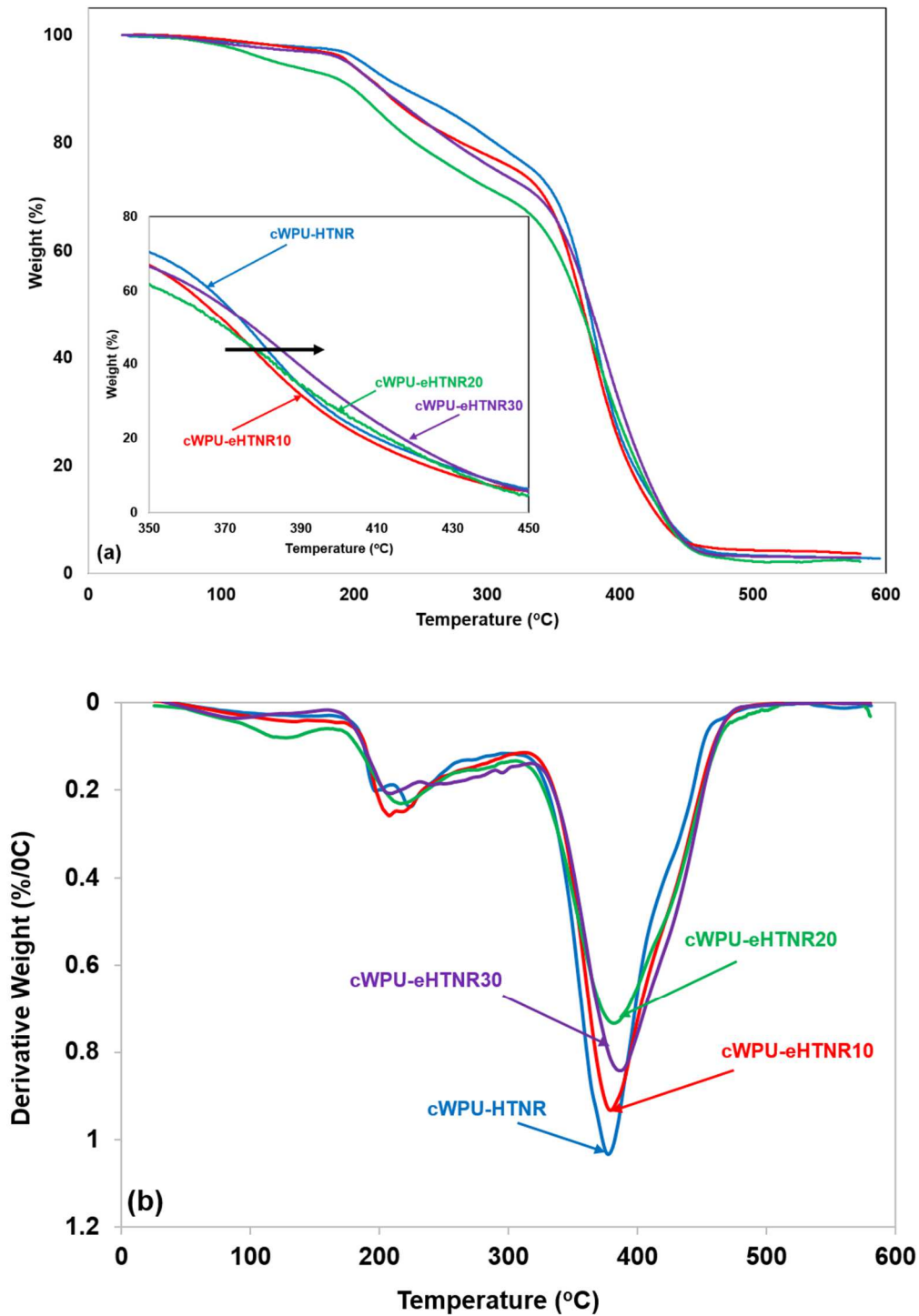


Figure 11. Thermograms for a series of cWPU-eHTNR films –)A(TGA curves, and)B(DTG curves.

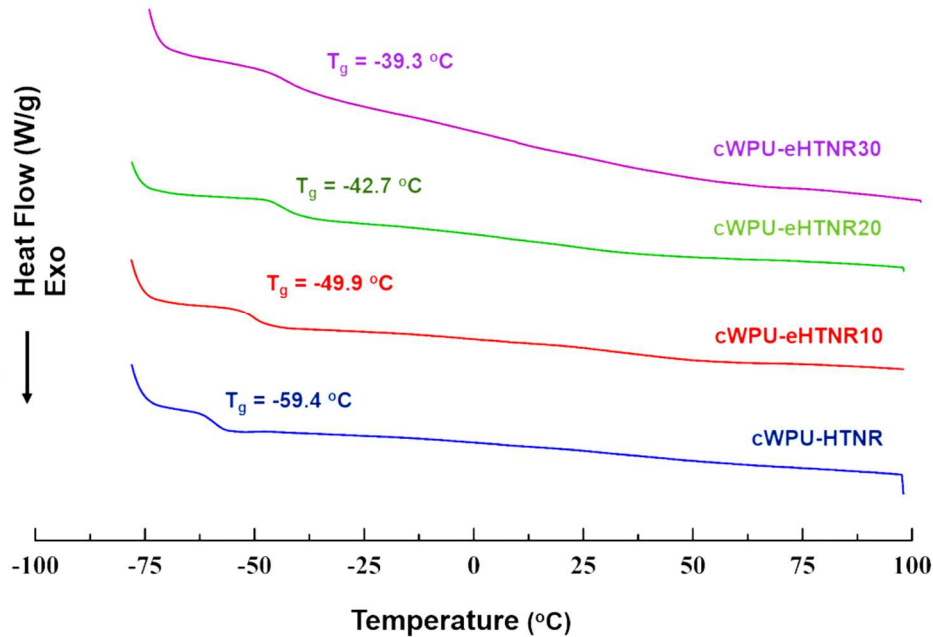


Figure 12 DSC thermograms for a series of cWPU-eHTNR films

Similar results are seen in dynamic mechanical properties. The evolution of storage modulus G' and $\tan \delta$ of cWPU-eHTNR films with proportion of epoxide units is presented against temperature. The curves of G' shift to higher values with epoxide content increase, as shown in **Figure 13) a**(. In addition, $\tan \delta$ peak of cWPU shifted to higher temperatures as shown in **Figure 13) b**(. These show that increasing epoxide content increased rigidity of structure, gave more interactions in the matrix, and increase energy dissipation. This indicates that the dynamic mechanical properties of cWPU films can be improved by increasing epoxide content on the main chain of HTNR polyol.

3.4 Electric Properties

There are many studies on the dielectric properties of thermoplastic polyurethane, one of the most promising types of dielectric elastomeric materials. It is reported that thermoplastic

polyurethane exhibits a large force output, a high dielectric constant, high mechanical properties and good mechanical strength] 36-38[. Prior to studying coating applications, dielectric properties and conductivity of our cWPU with epoxide modified HTNR were measured.

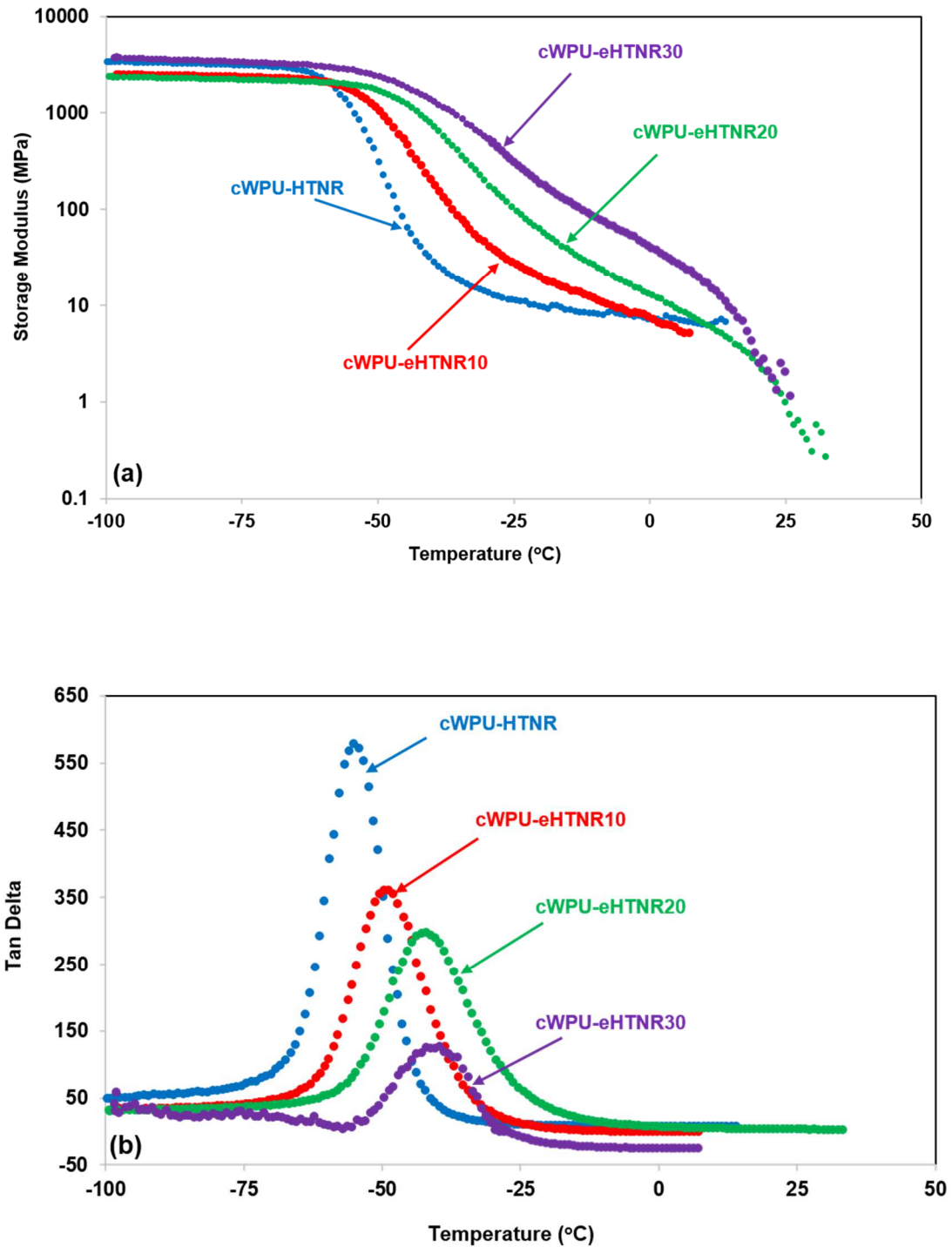


Figure 13 Storage modulus and Tan delta ($\text{Tan } \delta$) in a series of cWPU-eHTNR films

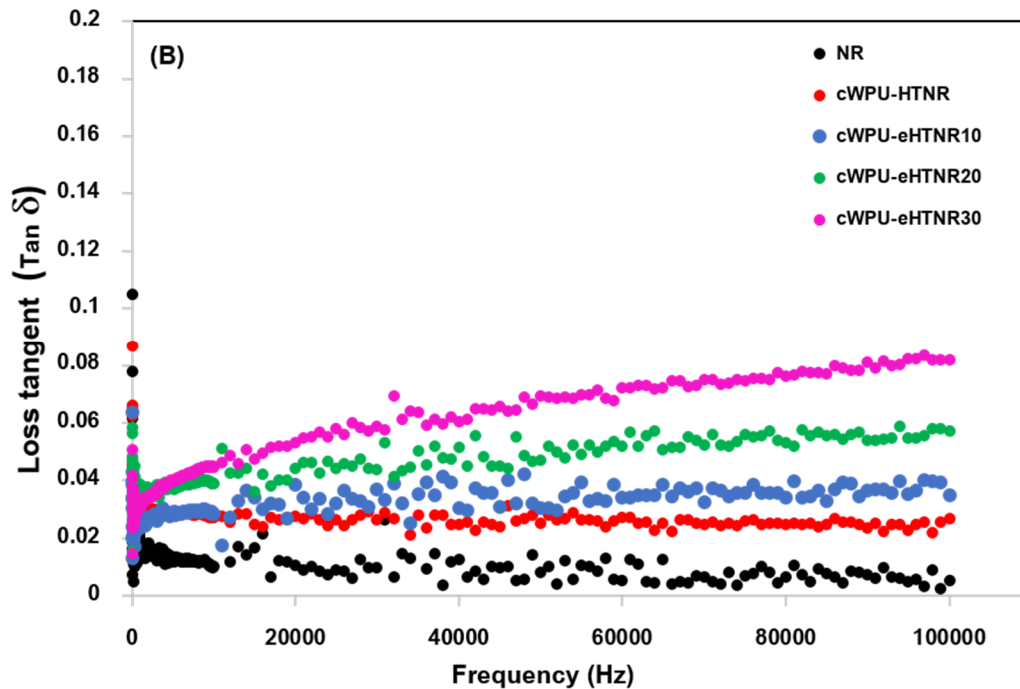
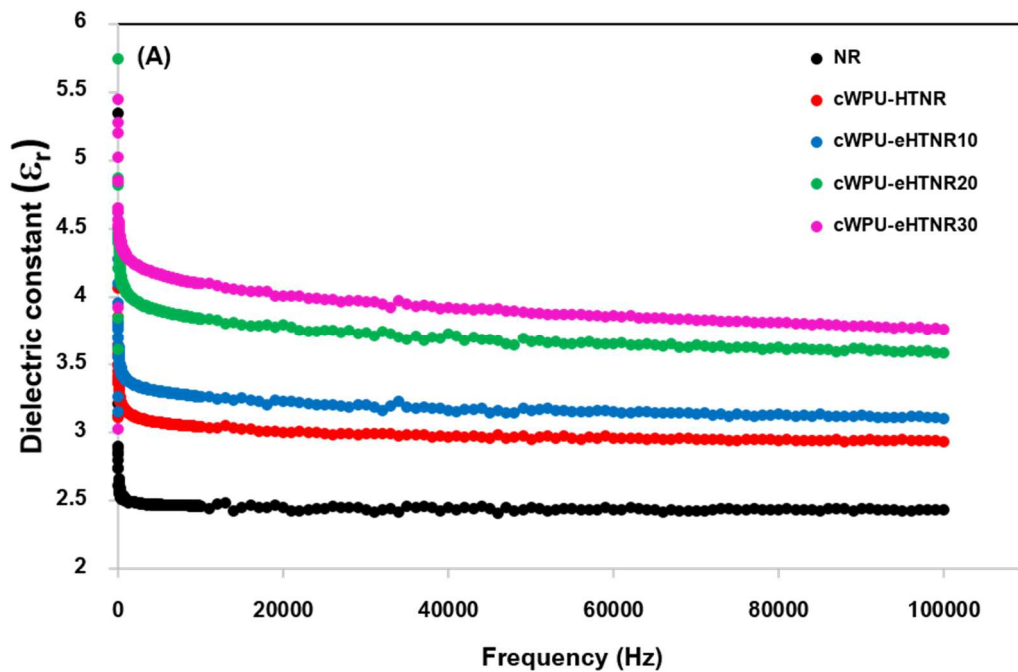


Figure 14)A(Dielectric loss, and)B(loss tangent in a series of cWPU-eHTNR films, in the frequency range from 0 to 100 kHz at room temperature.

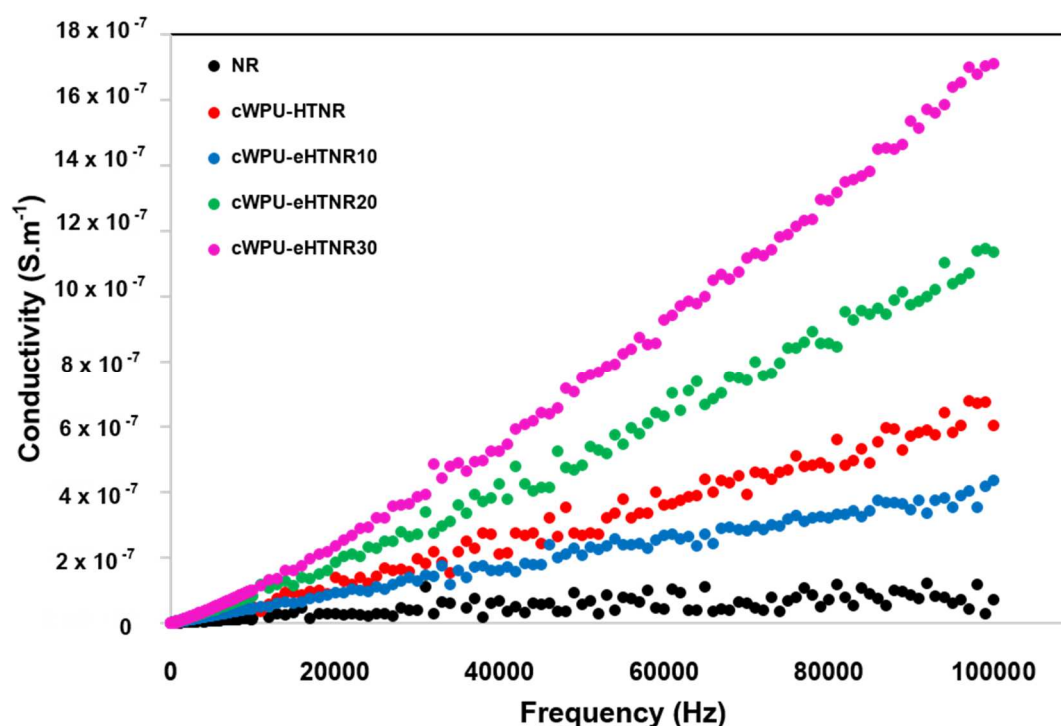


Figure 15. Conductivity in a series of cWPU-eHTNR films in the frequency range from 0 to 100 kHz at room temperature

The dielectric constant indicates strength of polarization in a material when exposed to an electric field] 39[. The results show that all of the cWPU films are typical dielectric materials. The film of plain NR had the least dielectric constant because there is no relevant functional groups in the main chain: the dielectric constant stems from other components, especially proteins]40-41[. These have a very low polarization, so the dielectric constant and the dielectric loss tangent are both very small. **Figure 14)A**(shows the dielectric constants of films in the cWPU series with different epoxide contents on HTNR from 0 to 30%. All of the films show slightly decreasing trend with frequency. In addition, the dielectric constant of cWPU films clearly increased with epoxide content in the main chain of cWPU. The dielectric constant increased from about 2.5 for plain NR to 3 and 4 for cWPU with epoxide contents from 0 to 30% . The strong frequency dependence of dielectric constants of WPU films is ascribed to charge polarization by electron delocalization in the main chains]42[.

Dielectric loss tangent of cWPU films and plain NR film as functions of frequency at room temperature are shown in **Figure 14)B**(. The trends resemble those of the dielectric constant. The dielectric loss increases with epoxide content in the backbone chain. The

epoxide structures can improve the polarization of cWPU in electric field, but it is not a good capacitor with easy release of electrons through the materials used.

The conductivities of all cWPU samples were measured as functions of frequency in the range from 0 to 100 kHz, and the results are shown in **Figure 15**. The conductivity of all the cWPU samples dramatically increased with frequency. Moreover, it can be observed that the conductivity increased with epoxide content. This can be attributed to the electron charges that can pass through the functional epoxide groups from chain to chain, much more easily than in other urethane groups. Also, the density of epoxide can help improve the localization of electrons. Therefore, the results show that conductivity increased with epoxide content. Even though the conductivity of these cWPU samples can be increased by increasing epoxide content, all the cWPU films show relatively low conductivities)lower than 10^{-6} S.m^{-1} ([38].

From the results, the dielectric properties of the coating material depend on the dipole parts, such as urethane linkages and epoxide groups in the main structure. The cWPU-HTNR film showed the lowest dielectric properties, while functionalizing with epoxide units gave higher dielectric properties. This evidence indicates that epoxide groups on the cWPU backbone enhanced the dielectric properties and all the cWPU film samples were good electric insulators.

3.5 Peel Test Results

The adhesion force on a real work piece surface is an important characteristic) or criterion for choice(of a coating material. In this work, the T-peel test was used to assess adhesion on leather at 70 °C. The strength of adhesion fluctuated, as shown in **Figure 16**. Peel forces of cWPU adhesives based on HTNR, eHTNR10, eHTNR20, and eHTNR30 were 13.45, 26.60, 11.19 and 8.76 N, respectively, while the lap shear forces of commercial adhesives A and B were 4.32, and 2.72 N, respectively.

In T-peel test results, eHTNR10 had the highest peel strength on real cow leather, superior to HTNR, eHTNR20, and eHTNR30. The cWPU adhesive displayed typical rigid and brittle behavior with the higher epoxidation levels, and this degraded the adhesion. Therefore, the cWPU adhesives with 10% epoxide groups)eHTNR10(gave the highest T-peel strength with best balance of cohesive and adhesive forces. According to the SEM images in **Figure 10**, the cWPU- eHTNR10 film was the most rough with the highest tensile strength. The synthesized cWPU adhesives showed overall good adhesion in comparison to the commercial adhesives.

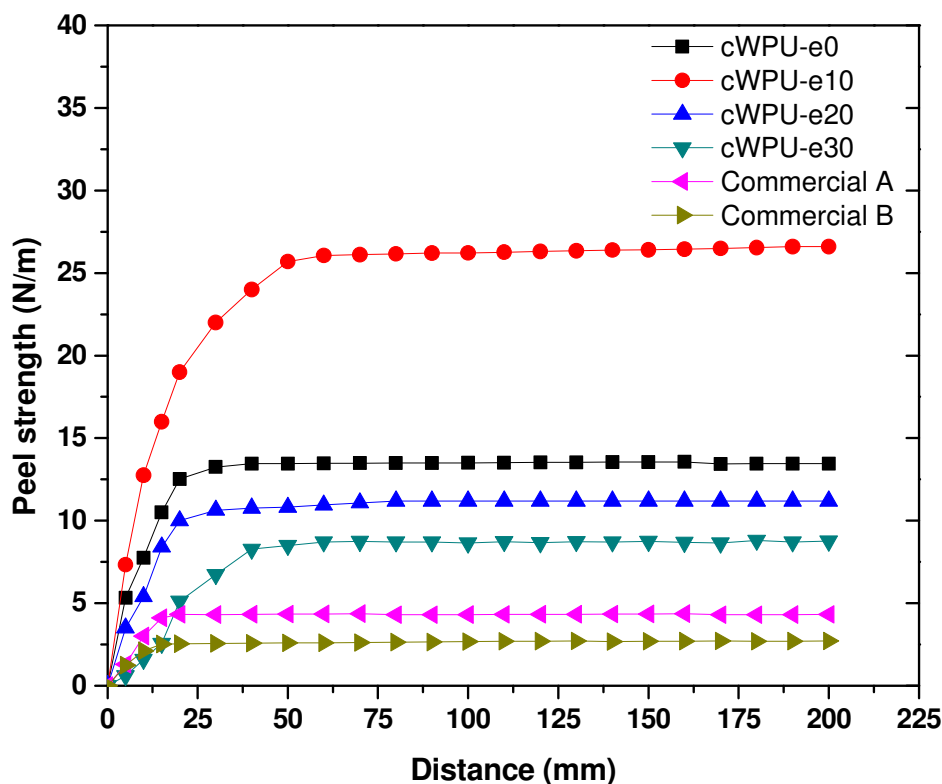


Figure 16. Peel strengths of a series of cWPU-eHTNR samples along with two commercial adhesives.

This study demonstrated that biosourced polyol based on eHTNR gave cWPU latex with good wettability, high thermal stability, and good adhesion properties. These have potential to serve various coating and adhesion applications.

4. Conclusions

Novel green high-adhesion coating materials from cWPU-eHTNR latex were successfully synthesized and had good storage stability with shelf-life exceeding 6 months. Epoxidation of HTNR backbone influenced the particle size distribution and the stability of cWPU latex: the particle size increased with epoxide content. All the stable cWPU-eHTNR latex showed monodisperse particle size distributions with low polydispersity index. In addition, epoxidation of HTNR increased polarity of cWPU-eHTNR films, leading to superior hydrophilicity, high surface free energy, good wettability, and good adhesion properties. Moreover, epoxidation of HTNR changed the elastic behavior towards rigid and

improved thermal stability of the cWPU-eHTRN films. In addition, cWPU-eHTNR films had low electric conductivity of a good insulator. The results revealed that cWPU-eHTNR10 latex had the highest potential for coating applications, and this cWPU-eHTNR also is an ecofriendly material based on a renewable resource.

Acknowledgments

This work was supported by Science Achievement Scholarship of Thailand; Natural Rubber Innovation Research Institute)Grant No. SCI581152S-0(; Research and Development Office)RDO()Grant No. MEDRU62057(; a scholarship was obtained for overseas thesis research from the graduate school of Prince of Songkla University, Thailand. At the Institut des Molécules et Matériaux du Mans, France, the authors wish to thank Sullivan Bricaud of the Nuclear Magnetic Resonance platform, for the NMR spectra; Anthony Rousseau of the Electronic microscopy platform, for taking the TEM images; Alexandre Benard and Mireille Barthe for the size exclusion chromatography analyses. We would like to thank the RDO and Assoc. Prof. Seppo Karrila for assistance with manuscript preparation.

References

1. Nakano, Y.; Okawa, K.; Nishijima, W.; Okada, M., Ozone decomposition of hazardous chemical substance in organic solvents. *Water Res.* **2003**, *37* (11), 2595-2598.
2. Noble, K.-L., Waterborne polyurethanes. *Prog. Org. Coat.* **1997**, *32* (1-4), 131-136.
3. Liu, H.; Li, C.; Sun, X. S., Soy-oil-based waterborne polyurethane improved wet strength of soy protein adhesives on wood. *Int. J. Adhes. Adhes.* **2017**, *73*, 66-74.
4. Lu, Y.; Larock, R. C., Soybean oil-based, aqueous cationic polyurethane dispersions: Synthesis and properties. *Prog. Org. Coat.* **2010**, *69* (1), 31-37.
5. El-Sayed, A. A.; Kantouch, F. A.; Kantouch, A., Preparation of cationic polyurethane and its application to acrylic fabrics. *J. Appl. Polym. Sci.* **2011**, *121* (2), 777-783.
6. Lai, X.; Song, Y.; Liu, M., Preparation and application of cationic blocked waterborne polyurethane as paper strength agent. *Journal of Polymer Research* **2013**, *20* (8), 1-6.
7. Li, J.; Zhang, X.; Gooch, J.; Sun, W.; Wang, H.; Wang, K., Photo- and pH-sensitive azo-containing cationic waterborne polyurethane. *Polym. Bull.* **2015**, *72* (4), 881-895.

8. Xin, H.; Shen, Y.; Li, X., Novel cationic polyurethane-fluorinated acrylic hybrid latexes: Synthesis, characterization and properties. *Colloids and Surfaces A: Physicochemical and Engineering Aspects* **2011**, *384* (1–3), 205-211.
9. Cheng, J.; Tang, X.; Zhao, J.; Shi, T.; Zhao, P.; Lin, C., Multifunctional cationic polyurethanes designed for non-viral cancer gene therapy. *Acta Biomaterialia* **2016**, *30*, 155-167.
10. Lu, Y.; Larock, R. C., Soybean-Oil-Based Waterborne Polyurethane Dispersions: Effects of Polyol Functionality and Hard Segment Content on Properties. *Biomacromolecules* **2008**, *9* (11), 3332-3340.
11. Ni, B.; Yang, L.; Wang, C.; Wang, L.; Finlow, D. E., Synthesis and thermal properties of soybean oil-based waterborne polyurethane coatings. *J. Therm. Anal. Calorim.* **2010**, *100* (1), 239-246.
12. Man, L.; Feng, Y.; Hu, Y.; Yuan, T.; Yang, Z., A renewable and multifunctional eco-friendly coating from novel tung oil-based cationic waterborne polyurethane dispersions. *J. Clean. Prod.* **2019**, 118341.
13. Liu, K.; Zhang, S. P.; Su, Z. G.; Ma, G. H., Preparation and Characterization of Castor Oil-Based Cationic Waterborne Polyurethane. *Advanced Materials Research* **2015**, *1090*, 3-7.
14. Saetung, A.; Rungvichaniwat, A.; Campistrone, I.; Klinpituksa, P.; Laguerre, A.; Phinyocheep, P.; Pilard, J. F., Controlled degradation of natural rubber and modification of the obtained telechelic oligoisoprenes: Preliminary study of their potentiality as polyurethane foam precursors. *J. Appl. Polym. Sci.* **2010**, *117* (3), 1279-1289.
15. Klinklai, W.; Kawahara, S.; Mizumo, T.; Yoshizawa, M.; Sakdapipanich, J. T.; Isono, Y.; Ohno, H., Depolymerization and ionic conductivity of enzymatically deproteinized natural rubber having epoxy group. *Eur. Polym. J.* **2003**, *39* (8), 1707-1712.
16. Sukhawipat, N.; Saetung, N.; Pilard, J.-F.; Bistac, S.; Saetung, A., Synthesis and characterization of novel natural rubber based cationic waterborne polyurethane—

- Effect of emulsifier and diol class chain extender. *J. Appl. Polym. Sci.* **2017**, *135*, 45715 (1 - 12).
17. Hu, H.; Yuan, Y.; Shi, W., Preparation of waterborne hyperbranched polyurethane acrylate/LDH nanocomposite. *Prog. Org. Coat.* **2012**, *75* (4), 474-479.
 18. Saldanha, D. F. S.; Canto, C.; da Silva, L. F. M.; Carbas, R. J. C.; Chaves, F. J. P.; Nomura, K.; Ueda, T., Mechanical characterization of a high elongation and high toughness epoxy adhesive. *Int. J. Adhes. Adhes.* **2013**, *47*, 91-98.
 19. Alvarez, G. A.; Fuensanta, M.; Orozco, V. H.; Giraldo, L. F.; Martín-Martínez, J. M., Hybrid waterborne polyurethane/ acrylate dispersion synthesized with bisphenol A-glycidylmethacrylate (Bis-GMA) grafting agent. *Prog. Org. Coat.* **2018**, *118*, 30-39.
 20. Yong, Q.; Pang, H.; Liao, B.; Mo, W.; Huang, F.; Huang, H.; Zhao, Y., Preparation and characterization of low gloss aqueous coating via forming self-roughed surface based on waterborne polyurethane acrylate hybrid emulsion. *Prog. Org. Coat.* **2018**, *115*, 18-26.
 21. Sukhawipat, N.; Raksanak, W.; Kalkornsurapranee, E.; Saetung, A.; Saetung, N., A new hybrid waterborne polyurethane coating synthesized from natural rubber and rubber seed oil with grafted acrylate. *Prog. Org. Coat.* **2020**, *141*, 105554.
 22. Wu, G.-m.; Kong, Z.-w.; Chen, J.; Huo, S.-p.; Liu, G.-f., Preparation and properties of waterborne polyurethane/ epoxy resin composite coating from anionic terpene-based polyol dispersion. *Prog. Org. Coat.* **2014**, *77* (2), 315-321.
 23. Reghunadhan, A.; Datta, J.; Jaroszewski, M.; Kalarikkal, N.; Thomas, S., Polyurethane glycolysate from industrial waste recycling to develop low dielectric constant, thermally stable materials suitable for the electronics. *Arabian Journal of Chemistry* **2020**, *13* (1), 2110-2120.
 24. Horowitz, H. H.; Metzger, G., A New Analysis of Thermogravimetric Traces. *Anal. Chem.* **1963**, *35* (10), 1464-1468.
 25. Shah, A. -u. -H., Calculation of Activation Energy of Degradation of Polyaniline-Dodecylbenzene Sulfonic Acid Salts via TGA. *Journal of Scientific and innovative research* **2013**.

26. Lehman, N.; Yung-Aoon, W.; Songtipya, L.; Johns, J.; Saetung, N.; Kalkornsuraanee, E. , Influence of functional groups on properties of styrene grafted NR using glutaraldehyde as curing agent. *Journal of Vinyl and Additive Technology* 0 (0).
27. Kaya, I. ; Avci, A. , Synthesis, characterization, and thermal stability of novel poly(azomethine-urethane)s and polyphenol derivatives derived from 2,4-dihydroxy benzaldehyde and toluene-2,4-diisocyanate. *Mater. Chem. Phys.* **2012**, 133 (1), 269-277.
28. Zhang, N.; Zhou, X.; Quan, H.; Sekiya, A., Study on the synthesis of toluene-2,4-diisocyanate via amine and carbonyl fluoride. *J. Fluorine Chem.* **2015**, 178, 208-213.
29. Joseph, E.; Singhvi, G., Chapter 4 - Multifunctional nanocrystals for cancer therapy: a potential nanocarrier. In *Nanomaterials for Drug Delivery and Therapy*, Grumezescu, A. M., Ed. William Andrew Publishing: 2019; pp 91-116.
30. Packham, D. E., Surface energy, surface topography and adhesion. *Int. J. Adhes. Adhes.* **2003**, 23 (6), 437-448.
31. Lin, Y. H.; Liao, K. H.; Chou, N. K.; Wang, S. S.; Chu, S. H.; Hsieh, K. H., UV-curable low-surface-energy fluorinated poly(urethane-acrylate)s for biomedical applications. *Eur. Polym. J.* **2008**, 44 (9), 2927-2937.
32. Hwang, H.-D.; Kim, H.-J., UV-curable low surface energy fluorinated polycarbonate-based polyurethane dispersion. *J. Colloid Interface Sci.* **2011**, 362 (2), 274-284.
33. Çanak, T. Ç.; Serhatlı, I. E., Synthesis of fluorinated urethane acrylate based UV-curable coatings. *Prog. Org. Coat.* **2013**, 76 (2), 388-399.
34. Zheng, G.; Lu, M.; Rui, X., The effect of polyether functional polydimethylsiloxane on surface and thermal properties of waterborne polyurethane. *Appl. Surf. Sci.* **2017**, 399, 272-281.
35. Kébir, N.; Campistron, I.; Laguerre, A.; Pilard, J.-F.; Bunel, C.; Couvercelle, J.-P.; Gondard, C., Use of hydroxytelechelic *cis*-1,4-polyisoprene (HTPI) in the synthesis of polyurethanes (PUs). Part 1. Influence of molecular weight and chemical modification of HTPI on the mechanical and thermal properties of PUs. *Polymer* **2005**, 46 (18), 6869-6877.

36. Xiang, D.; Liu, M.; Chen, G.; Zhang, T.; Liu, L.; Liang, Y., Optimization of mechanical and dielectric properties of poly(urethane–urea) -based dielectric elastomers via the control of microstructure. *RSC Advances* **2017**, *7* (88), 55610-55619.
37. Lorenzini, R. G.; Kline, W. M.; Wang, C. C.; Ramprasad, R.; Sotzing, G. A., The rational design of polyurea & polyurethane dielectric materials. *Polymer* **2013**, *54* (14), 3529-3533.
38. Tian, M.; Yao, Y.; Liu, S.; Yang, D.; Zhang, L.; Nishi, T.; Ning, N., Separated-structured all-organic dielectric elastomer with large actuation strain under ultra-low voltage and high mechanical strength. *Journal of Materials Chemistry A* **2015**, *3* (4), 1483-1491.
39. Çelik, T.; Coşkun, M. F., Dielectric and thermal properties of the methacrylate polymer bearing chalcone side group. *J. Mol. Struct.* **2018**, *1157*, 239-246.
40. Gilson, M. K.; Honig, B. H., The dielectric constant of a folded protein. *Biopolymers* **1986**, *25* (11), 2097-2119.
41. Gramse, G.; Schönhals, A.; Kienberger, F., Nanoscale dipole dynamics of protein membranes studied by broadband dielectric microscopy. *Nanoscale* **2019**, *11* (10), 4303-4309.
42. Bánhegyi, G., Comparison of electrical mixture rules for composites. *Colloid. Polym. Sci.* **1986**, *264* (12), 1030-1050.